# Towards a Haptic Feedback Framework for Multi-DOF Robotic Laparoscopic Surgery Platforms

Adnan Munawar<sup>1</sup> and Gregory Fischer<sup>2</sup>

Abstract—The use of robotics for laparoscopic surgery has been an established field for over a decade. However, with the influx of advanced tools and algorithms for general purpose robotics, there is a need to incorporate these advancements into medical robotics technology. The daVinci Research Kit and its software framework provides a step towards these advancements. This paper presents the development of new tools and utilization of previously developed tools used for general purpose robotics, and their tailored use in medical robotics. Additionally, a method for computing haptic forces for tele-operated surgical robots is presented. The technique utilizes elastic, Spherical Proxy Regions (SPR) to readily compute directional interaction forces and manipulate them to create a dynamic behavior at the surgeon/user's manipulator.

#### I. INTRODUCTION

The origins of Robotic Laparoscopic Surgery date back to mid 1980's when PUMA 560 was used to perform a neurosurgical biopsy [1]. A few years following this procedure, the first robot was used to perform a cholecystectomy[2]; ultimately catalyzing the increase in robot-assisted surgeries throughout the late 80s and into the 90s[3][4]. Through the continued success of such surgeries, the use of robots for surgical use has proven to be advantageous over traditional laparoscopy, as it provides increased precision, ease of use, elimination of fatigue for labor-intensive movements in traditional laparoscopy, as well as motion scaling[5]. However, while this continued use of robots for laparoscopic surgeries has proven to be intrinsic in providing surgical precision, the loss of touch/haptics, non-stereoscopic view of the internal body, and reduced degrees of freedom pose to be significant areas of improvement which much be addressed for the continued success of robot-assisted surgeries[5].

The following years saw the development of several robotic surgery platforms such as Robodoc [6], Probot [3], Zeus etc. By the end of the 20th century, these technologies/platforms were either deprecated or merged into a single robotic platform know as the daVinci Surgical Robot [7]. The daVinci Surgical Robot gained FDA approval for lower abdominal laparoscopy in 2001 [5] and has since dominated the robot assisted surgical space.

Advancements in general purpose robotics and a more frequent release cycle of new software/hardware tools have increasingly made inroads for general purpose robotic in medical technology. We are certainly at the footsteps of the





Fig. 1: User holding an MTM on the right and two PSMs on the left.( dVRK setup at AIMLab, WPI)

dawn of a new age of medical intervention using robotic assistance.

This research focuses on the development and inclusion of several general purpose robotic tools tailored for application in medical robotics. More specifically, this research provides a study and implementation of a haptic feedback framework for tele-operated minimally invasive surgery. The study intends to take a step towards intelligent, generic and customizable solutions to address some of the key disadvantages associated with robot assisted surgery and haptics[8].

#### II. THE DAVINCI RESEARCH KIT

The daVinci Research Kit (dVRK) setup AIM Labs is shown in Figure 1. The dVRK includes the clinical daVinci Surgical Robot (Master Tool Manipulators (MTM), Patient Side Manipulators (PSM), Endoscopic Camera Manipulator (ECM) and the footpedal tray) without the proprietary controllers and software. PSMs and the ECM are kinematically similar and are teleoperated by the surgeon using MTMs and the footpedal tray, allowing clutch based engagement.

Custom controllers and software had to developed to control the dVRK components. John Hopkins University (JHU) led this effort [9][10] and choose an open source architecture for the controllers(based on FGPA-1394/QLA design) and the software(CISST/SAW libraries). While this control architecture forms the low level control of the dVRK, a significant amount of work has been done afterwards to include general purpose and modern robotics tools, predominantly focusing on building a ROS interface.

The ROS interface forms the high level control architecture and allows the inclusion of a variety of advanced simulation tools. A motion planning framework for the

<sup>&</sup>lt;sup>1</sup>Adnan Munawar is a PhD student at Worcester Polytechnic Institute, Worcester, MA 01609, USA amunawar@wpi.edu

<sup>&</sup>lt;sup>2</sup>Gregory S. Fischer is with the Faculty of Mechanical Engineering and Robotics Engineering at Worcester Polytechnic Institute, Worcester, MA 01609, USA gfischer@wpi.edu

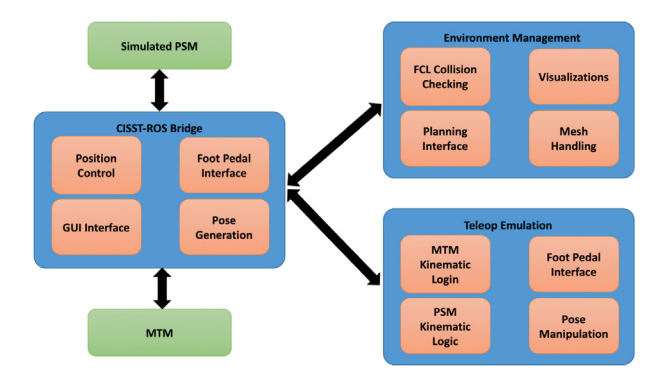


Fig. 2: Figure showing the general outline of the Motion Planning Framework. The MTM teleoperates the PSM through the core packages under the cisst-ROS bridge and TeleOp Emulation namespace. Motion planning and collision checking tasks are performed by packages under than environment management namespace

dVRK [11] is one such example of the utilization of ROS with dVRK. This tool allows the intelligent manipulation of PSMs in simulated and real environments.

#### A. Manipulation inside Simulated Environment

The motion planning framework for dVRK has been implemented using a combination of both native and self-created ROS tools. Such an implementation has been aided by the hierarchical control architecture, thus performing high level algorithmic tasks using node-based ROS packages, while maintaining low latency and high bandwidth control of the actual manipulators.

The motion planning interface for the dVRK relies on MoveIt[12] and Fast Collision Library (FCL)[13]. The interface allows for the simulation, sensing and planning inside virtual environments. The ultimate goal is to replicate simulated environments with actual environments, streamed as point cloud data, while successively performing sensing and manipulation.

For the current system, a mesh can be visualized in the planning environment and collisions can be retrieved using FCL, Figure 3b. The fast and visual collision check is useful for motion planning tasks for tele-operating PSMs in simulated environment. An extrapolation of this tool is to generate haptic feedback when PSM comes in contact with the environment. To allow for the tele-operation of the simulated PSMs using actual MTMs, the interface shown in Figure 2 has been developed. Figure 2 demonstrates a modular node based design with packages categorized in 3 different name-spaces, highlighting their utility. Such a node based design is the backbone of this research which is presented in the remaining paper. A collision detection with a virtual environment is demonstrated in Figure 3.

# III. NEED FOR HAPTIC FEEDBACK

One of the major disadvantage of robot assisted laparoscopy is the loss touch. While there hasn't been a conclusive study to prove its effectiveness, it is generally believed

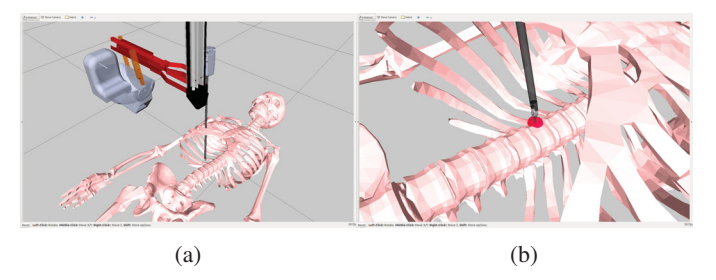


Fig. 3: A 3D volumetric skeletal mesh is loaded as an environment. Figure (b) shows the collision point when the PSM interacts with the skeletal mesh

that such a feature would enhance the surgical procedure as argued in [14][15]. As a result, research has been focused towards achieving haptic feedback in teleoperated surgical test cases. Among many others, Okamura [16], Ryden et al [17] and Westebring et al [18] are notable for their research in the field of surgical haptics. Ryden presents a novel proxy based approach towards haptic feedback, where a deflection from a proxy region is used to compute haptic feedback.

In general, the research towards haptic feedback has been evaluated using commercially available devices (e.g. Falcon and Phantom haptic devices). This research, however, is focused on implementing haptic feedback on the Master Manipulator of the surgical robot itself. As opposed to the commercially available systems, the inertial parameters of the master manipulator pose a major challenge to achieve a reliable haptic feedback.

#### A. Problem Formulation

In robot assisted teleoperated laparoscopy the physical segregation between the MTM and the PSM takes away direct force interaction. To compute an interaction force at the MTM, a simulated environment replicating the actual surgical area is created. The simulated PSMs are then teleoperated via actual MTMs using the interface shown in Figure 2

Once the simulated PSMs come in contact with the collision environment, a haptic force needs to be computed that acts on the surgeon/users hand (via the MTM) to get a sense of the environment being interacted with. The computation of the haptic force and the interaction control of the MTM are seperate problems. Haptic force computation requires the analysis of topological contact of the PSMs with the environment[19] while interaction control requires the computation of the dynamics of the MTM.

The first problem in computing haptic force is that the collision checking using FCL only provides the points where the collision occurs and not the explicit information of the contact normals. A trivial solution to get the contact normals is to explicitly compute the normals of the entire mesh environment. Consequently, the normal vector(s) corresponding to the collision point(s) can be retrieved and directional forces can be generated. This approach requires pre-computation and storage of normals for the collision mesh which is both computationally demanding and requires

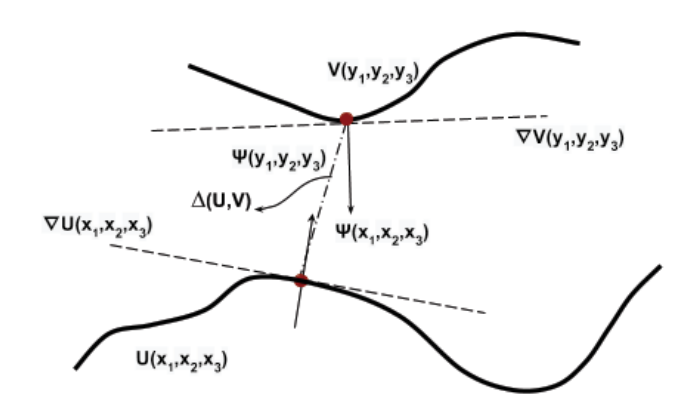


Fig. 4: The relation between the surface normals  $\psi(x_1^\star, x_2^\star, x_3^\star)$  and  $\psi(y_1^\star, y_2^\star, y_3^\star)$  as the two continuously differentiable parameteric surface  $U(x_1, x_2, x_3)$  and  $V(y_1, y_2, y_3)$  approach each other while minimizing  $\Delta(U, V)$ 

modifications to the established framework for dVRK and MoveIt.

A different approach of generating contact normals with collision surfaces is presented in the next section. The second problem dealing with the computation of the haptic feedback requires the knowledge of the arm dynamics and a developing a control methodology for regulating forces on the MTM. This is presented in section IV.

# B. Generation of Normal Forces on Point Contact

As the PSM comes in contact with the environment, the FCL collision checking library provides points at which the collision occurs. These points by themselves cannot be used to generate normal forces as the direction of the force vector is unknown. One approach to address the problem is to use the direction of velocity of the PSMs end-effector, v, just before the collision occurred. It can be shown that such an approach only works for cases in which the direction of approach of the PSM is normal to the surface. For different angles of approach, the direction of feedback force is not normal to the collision surface. The problem in this case is addressed using concepts from geometry, presented as follows.

#### C. Point Contact between Two Surfaces

Consider a continuously differentiable, parametric surface U defined as:

$$U = ax_1^m + bx_2^n + cx_3^o (1)$$

The function U maps each point in surface to SE(3) space. The surface gradient of U yields the surface normal to any given point.

$$\psi(x_1, x_2, x_3) = \nabla U = \frac{\delta U}{\delta x_1} \epsilon_{x1} + \frac{\delta U}{\delta x_2} \epsilon_{x2} + \frac{\delta U}{\delta x_3} \epsilon_{x3} \quad (2)$$

Where  $\epsilon_{x1}=\begin{bmatrix}1&0&0\end{bmatrix}$ ,  $\epsilon_{x2}=\begin{bmatrix}0&1&0\end{bmatrix}$  and  $\epsilon_{x3}=\begin{bmatrix}0&0&1\end{bmatrix}$ . Given a point of interest  $\rho^{\star}=(x_1^{\star},x_2^{\star},x_3^{\star})$  with

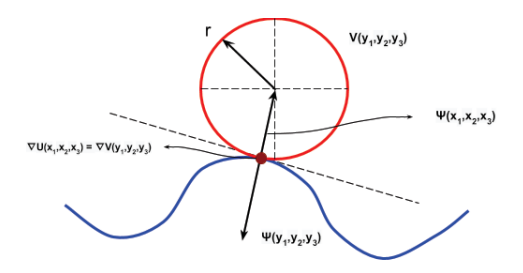


Fig. 5: Demonstration of collinearity of surface normals  $\nabla U(x_1, x_2, x_3)$  and  $\nabla V(y_1, y_2, y_3)$  at point contact.

the corresponding normal  $\psi(x_1^{\star}, x_2^{\star}, x_3^{\star})$ :

$$\psi(x_1^{\star}, x_2^{\star}, x_3^{\star}) = \nabla U^{\star} = U_{x_1}(x_1^{\star}) + U_{x_2}(x_2^{\star}) + U_{x_3}(x_3^{\star})$$
 (3)

the equation of a plane tangent to the point can be calculated as:

$$\psi(x_1^{\star})(x_1 - x_1^{\star}) + \psi(x_2^{\star})(x_2 - x_2^{\star}) + \psi(x_3^{\star})(x_3 - x_3^{\star}) = 0$$
 (4)

Now consider a secondary, continuously differentiable, parametric surface V, the normal to which can be computed in a similar fashion to eq. 2.

$$\psi(y_1, y_2, y_3) = \nabla V = \frac{\delta V}{\delta y_1} \epsilon_{y1} + \frac{\delta V}{\delta y_2} \epsilon_{y2} + \frac{\delta V}{\delta y_3} \epsilon_{y3}$$
 (5)

At a point of interest  $\rho^* = (y_1^*, y_2^*, y_3^*)$  with the normal  $\psi(y_1^*, y_2^*, y_3^*)$ , the corresponding tangent plane is expressed as:

$$\psi(y_1^{\star})(y_1 - y_1^{\star}) + \psi(y_2^{\star})(y_2 - y_2^{\star}) + \psi(y_3^{\star})(y_3 - y_3^{\star}) = 0$$
 (6)

. If the two surfaces U and V, shown in Figure 4, approach towards each other such that  $\Delta(U,V)$  approaches zero then at the point contact, their surface normals  $\psi(x_1^\star,x_2^\star,x_3^\star)$  and  $\psi(y_1^\star,y_2^\star,y_3^\star)$  should become collinear. This condition is explored in Lemma below.

**Lemma 1.** For two continuously differentiable, parametric surfaces, represented by  $U(x_1, x_2, x_3)$  and  $V(y_1, y_2, y_3)$  having normals  $\psi(x_1, x_2, x_3)$  and  $\psi(y_1, y_2, y_3)$  respectively. At any point contact  $p^*$ , their normals  $\psi(x_1^*, x_2^*, x_3^*)$  and  $\psi(y_1^*, y_2^*, y_3^*)$  are collinear to each other.

*Proof.* By contradiction, if the two normals  $\psi(x_1^\star, x_2^\star, x_3^\star)$  and  $\psi(y_1^\star, y_2^\star, y_3^\star)$  are not collinear to each other at a contact point  $\rho^\star$ , we shall have two non coplanar tangential planes at the point  $\rho^\star$ . This means that for each surface U and V, there exist two different tangential planes at the point  $\rho^\star$ . This is mathematically impossible by the definition of tangent planes along a continuously differentiable surface. Thus Lemma 1 is proved.

#### D. Generation of a CPR around the PSMs End-Effector

Using the discussion and proof in section III-C and a few geometrical concepts, the problem encountered in section III-B can be addressed as follows.

Consider a sphere (for which all the normals at the circumference pass through the center) as a proxy (Figure 5).

This proxy, positioned at the tip of the PSM, is referred to as a spherical proxy region (SPR). Whenever a collision occurs between this sphere and the environment, a collision point can be collected using FCL. Using Lemma 1 it can be argued that for the SPR, the contact normal passes through its center. Hence we can readily get the direction of normal along which the contact occurs by taking the vector difference between the collision point and the centroid of the SPR.

# E. Dynamic Haptic Model

For haptic feedback during teleoperation, the SPR is modelled with an elastic spring and damper as shown in Figure 6. The spring K and the damper B are essentially multi-dimensional mapping functions, providing stiffness and damping in Cartesian space. The penetration of the SPR in the environment causes a force to emanate at the tip of the PSM as shown in Figure 8.

$$F_{haptic} = H_{ps}^{mb}(q)K\partial(x) + H_{ps}^{mb}(q)B\partial(\dot{x})$$
 (7)

In equation 7, a spatial force at the PSM is expressed in Body Frame of the MTM,  $H_{ps}^{ms}$  is the constant transformation between the PSMs and MTMs Base frame and  $H_{ms}^{mb}(q)$  is the transformation between MTMs Base frame and Tip frame. The transformation  $H_{ms}^{mb}(q)$  is the function of  $\mathbf{q}=(q_1,q_2,...,q_7)^T$ , the MTM joint angles.

$$H_{ps}^{mb}(q) = H_{ms}^{mb}(q)H_{ps}^{ms}$$
 (8)

In equation 7, K and  $B \in \mathbb{R}^{3\times3}$  diagonal matrices:

$$K = \begin{bmatrix} K_{y1} & 0 & 0 \\ 0 & K_{y2} & 0 \\ 0 & 0 & K_{y3} \end{bmatrix} B = \begin{bmatrix} B_{y1} & 0 & 0 \\ 0 & B_{y2} & 0 \\ 0 & 0 & B_{y3} \end{bmatrix}$$
(9)

# IV. MODELLING CONTACT DYNAMICS AROUND SPHERICAL PROXY REGION

### A. Classification of the Haptic Interaction for the MTM

The haptic interaction of the MTM when the teleoperated PSM interacts with the environment can be classified as either Admittance Control or Impedance Control. In Impedance control, an input deflection in position results in the computed force as output, while in Admittance control, an input force results in a deflection of position as the output. Hogan argued that for any interaction of a manipulator with the environment, the manipulator be treated as Impedance and the environment as Admittance while Newman suggested vice-versa. For the dVRKs use case, the haptic feedback at the MTM can be readily classified as an additional force at the end-effector. This classification leads towards Impedance control. Implementation wise, a specialized impedance controller is proposed, with just the proportional and damping gains. Such a control scheme is classified in literature as stiffness control [20].

Consider the general dynamics equation of a manipulator.

$$M(q)\ddot{q} + C(q,\dot{q})\dot{q} + G(q) = \tau - \tau_e \tag{10}$$

Where  $M(q) \in \mathbb{R}^{n \times n}$  is the Inertia matrix,  $C(q, \dot{q}) \in \mathbb{R}^{n \times n}$  is the Coriolis matrix,  $G(q) \in \mathbb{R}^{n \times 1}$  Gravitational

vector and  $\tau \in \mathbb{R}^{n \times 1}$  and  $\tau_e \in \mathbb{R}^{n \times 1}$  the dynamic and external torque on the manipulator. Equation 10 provides the dynamic behavior of the system in joint space. A more useful approach is to convert this dynamic equation into Cartesian space. Using the Jacobain  $J(q) \in \mathbb{R}^{n \times p}$  and some pre and post multiplication of the terms of M(q),  $C(q,\dot{q})$  and G(q), we arrive at the following dynamic equation representing the system dynamics in Cartesian space.

$$\Lambda(q)a + \Gamma(q,\dot{q})v + \eta(q) = F - F_e \tag{11}$$

In equation 11, a and v represent the instantaneous Cartesian acceleration and velocity of the end-effector. The remaining terms are evaluated as follows:

$$\Lambda(q) = (J(q)M(q)^{-1}J(q)^{T})^{-1} \tag{12}$$

$$\Gamma(q) = J(q)^{-T} C(q, \dot{q}) J(q)^{-1} - \Lambda(q) J(q) J(q)^{-1}$$
 (13)

$$\eta(q) = J(q)^{-T}G(q) \tag{14}$$

It is important to point out that the conversion from Joint Space to Cartesian Space requires the pre and post multiplication of the Inverse of the Jacobian with the Inertia, Coriolis and Gravity Matrices. For this, the Jacobian has to be a non-singular square matrix. Kinematically speaking, either a 3 DOF planar manipulator or 6 DOF spatial manipulator satisfies the criteria for the inverse of the Jacobian to hold. MTMs on the other hand are 7 DOF manipulators, hence only the pseudo inverse of the Jacobain can be taken. One way to avoid taking the pseudo inverse is to distribute the kinematics of the MTM and consider its first three links only. This allows for just the external forces  $F_e = [F_{xe}F_{ye}F_{ze}]'$  to be included in the dynamic model while ignoring the endeffector torques  $T_e = [T_{xe}T_{ye}T_{ze}]'$ . From the perspective of haptic feedback, this meets the minimum criteria for interaction control.

 $F_{haptic}$  can be incorporated with equation 11 to create the full haptic feedback equation for the MTM.

$$\Lambda(q)a + \Gamma(q,\dot{q})v + \eta(q) = F - H_{ms}^{mb}(q)^{-1}F_{hantic}$$
 (15)

#### B. Implementation Details

Most of the dynamic components of the MTM are unknown. A regression approach has been used to evaluate just the gravitational torques. By collecting the known parameters from the unknowns, the gravitational torques can be estimated as follows:

$$\eta(q) = -\frac{d}{dt}\frac{\partial(P)}{\partial(\dot{q})} + \frac{\partial(P)}{\partial(q)} \tag{16}$$

$$\frac{d}{dt}\frac{\partial(P)}{\partial(\dot{q})} - \frac{\partial(P)}{\partial(q)} \approx -\Upsilon(q, \dot{q}, \ddot{q})\Pi; \quad \Upsilon \in \mathbb{R}^{n \times p}$$
 (17)

$$\Pi_E = -\Upsilon(q, \dot{q}, \ddot{q})^{\dagger} \bar{T}(q); \quad \Pi_E \in \mathbb{R}^{p \times 1}$$
 (18)

In equation 18,  $\Pi_E$  is vector of estimated parameters using the manual calibration of torques  $\bar{T}(q) \in \mathbb{R}^{n \times 1}$  at different

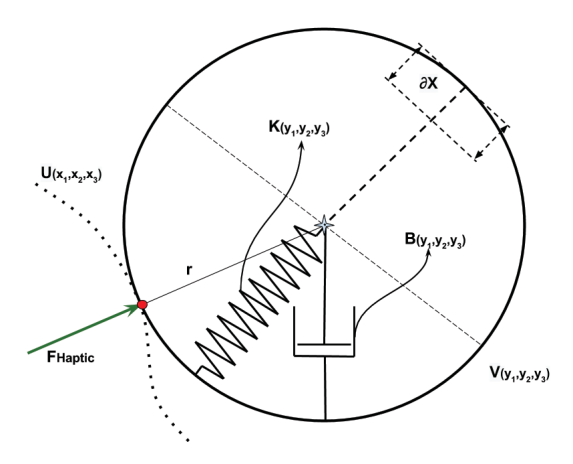


Fig. 6: Generalization of the SPR for 2-D with an elastic and damping element. The springs active length is related to the radius of the SPR.

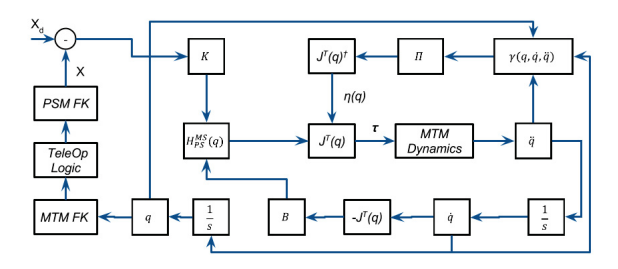


Fig. 7: A simplified block diagram representing the Stiffness Control with Gravity Compensation for the haptic feedback framework

configurations, keeping the arm stationary with minimum effort.

For special scenarios in which the environment is static, the desired velocity in equation 7 is set to zero so that the goal of B is to minimize the residual velocity when a contact between the SPR and the environment happens. Additionally, for cases involving the motion of the MTM with minute endeffector acceleration and velocities and considering equation 17, equation 15 leads to equation 19.

$$F = (J(q)^T)^{\dagger} \Upsilon(q, \dot{q}, \ddot{q}) \Pi_E + H_{ps}^{ms}(q) (K \partial x - B \dot{x}) \quad (19)$$

The high level control loop for haptic feedback is set to run at 500 Hz, with a consistent update rate to the MTM controllers. The low level torque controller runs at a much higher speed (> 2Khz) and maintains the torque in between the update cycles of haptic feedback. Higher speeds are possible but have not been tested yet. The collision update rate is set to run at 250 Hz. A block diagram for the control scheme is shown in Figure 7.

# V. RESULTS AND DISCUSSION

The experimental setup consists of one PSM in simulation being teleoperated by an actual MTM. The PSM follows



Fig. 8: Figure showing the deflection response and consequently the computed force as the penetration depth of the SPR increases

all the control protocols that the actual PSM follows in teleoperation mode (engaging/disengaging movements on pressing foot pedals). The diameter of the SPR is 30 mm, K = diag(200, 200, 200) and B = diag(10, 10, 30). As the PSM moves into the collision environment, a collision is detected and the SPR is used to generate a collision normal at that point. This gives the direction of the force, while the penetration of the SPR inside the collision environment is used to calculate the deflection  $\partial x$ , the penetration velocity  $-\dot{x}$  is the current velocity of any point inside the SPR. It can be seen in the Figures 9(a)-(c) that a normal force is computed at this point according to equation 7. In Figures 9 (d)-(f), two wrenches are visualized for the MTM, Spatial Wrenches are represented by green arrows and Body or Tool Wrenches in red. At the MTM, the body wrench is continually mapped to spatial wrench using equation 8.

This research is a step towards implementation of haptics for surgical robotics using generic tools. The contribution is geared towards using the actual surgical manipulators rather than off-the-shelf haptic devices and proprietary software. The concept of a spherical proxy region allows for the computational economy and a dynamic behavior of the interaction environment.

It should be noted that the selection of the diameter of the SPR is dependent upon the required clearance of the slave manipulators tip with the environment and the topological detail. Environment with finer details would require a smaller radius of the SPR, however, a smaller radius would induce noise in the direction of the haptic force. For such scenarios, a filter on the output of the haptic force is proposed.

For the cases shown in Figure 9, the environment meshes have a relatively high number of faces. This requirement is based of the discussion presented in section III-C. This is a drawback to the algorithm in its current implementation. For a surface with lower number of mesh faces compared to its curvature, sudden changes in the mesh normals will occur. This will result is jagged output of the Haptic Force. This problem can be addressed by using a filter to smooth out the computed normals and a topic of further research.

The haptic feedback at the MTM acts as 3 dimensional, linear spring with added damping. As the SPR penetrates into a collision environment, the elastic behaviour of the MTM might be feasible for some cases. However, for other cases, a more appropriate interaction could be stiff wall that the MTM is forbidden to penetrate through. This is a further area of research and would rely on the review and study of the interaction schemes that a user experiences while

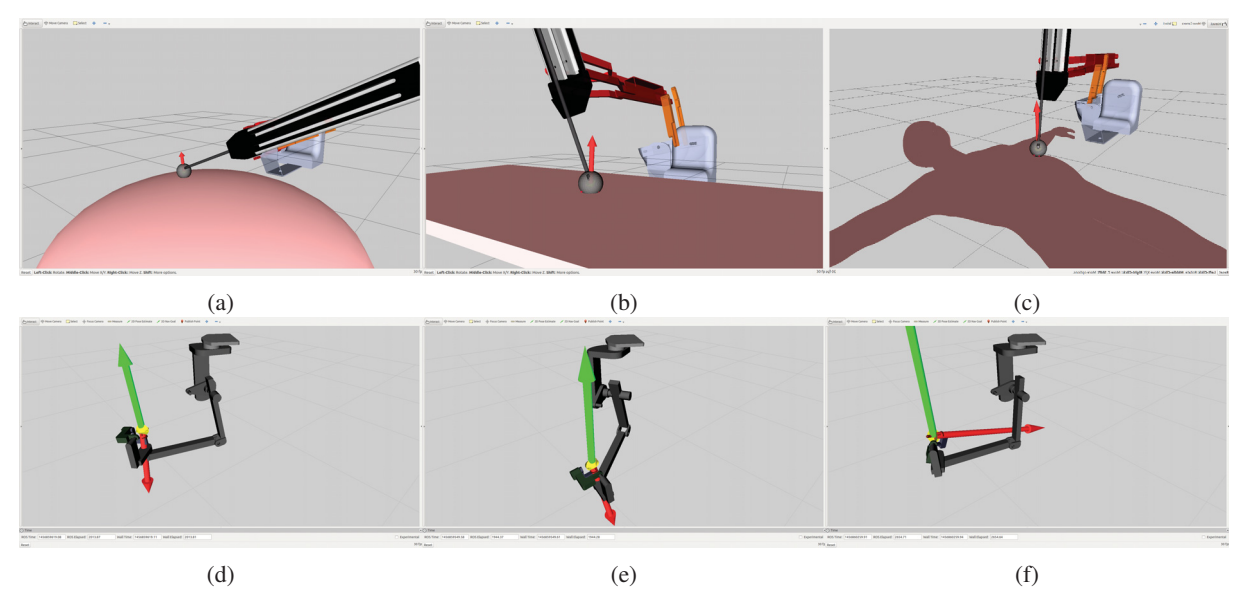


Fig. 9: The pair of Figures for each column demonstrate the interaction of the PSM with a different mesh and the corresponding haptic forces on the MTM

manipulating objects in real life. The work of Colgate [21] provides an interesting insight into this, however most of the existing research deals with haptic devices that have low mass properties and are designed with the intended uses case of haptic interaction. Dealing with generic manipulators and tuning the response to provide appropriate interaction is a challenging task and a focus of this research.

#### REFERENCES

- [1] Yik San Kwoh, Joahin Hou, Edmond A Jonckheere, and Samad Hayati. A robot with improved absolute positioning accuracy for CT guided stereotactic brain surgery. *Biomedical Engineering, IEEE Transactions on*, 35(2):153–160, 1988.
- [2] Michel Gagner, Eric Begin, Richard Hurteau, and Alfons Pomp. Robotic interactive laparoscopic cholecystectomy. The Lancet, 343(8897):596–597, 1994.
- [3] BL Davies, RD Hibberd, MJ Coptcoat, and JEA Wickham. A surgeon robot prostatectomy-a laboratory evaluation. *Journal of medical engineering & Damp; technology*, 13(6):273–277, 1989.
- [4] Richard M Satava. Robotic surgery: from past to future—a personal journey. Surgical Clinics of North America, 83(6):1491–1500, 2003.
- [5] VR Patel, MF Chammas, and S Shah. Robotic assisted laparoscopic radical prostatectomy: a review of the current state of affairs. *Inter*national journal of clinical practice, 61(2):309–314, 2007.
- [6] Richard M Satava. Surgical robotics: the early chronicles: a personal historical perspective. Surgical Laparoscopy Endoscopy & Company Percutaneous Techniques, 12(1):6–16, 2002.
- [7] The Economist Online. Surgical Robots: The kindness of strangers. http://www.economist.com/blogs/babbage/2012/01/surgicalrobots, Jan 2012.
- [8] Charles L Bennett, Steven J Stryker, M Rosario Ferreira, John Adams, and Robert W Beart. The learning curve for laparoscopic colorectal surgery: preliminary results from a prospective analysis of 1194 laparoscopic-assisted colectomies. Archives of Surgery, 132(1):41–44, 1907
- [9] M Jung, T Xia, A Deguet, R Kumar, R Taylor, and P Kazanzides. A surgical assistant workstation (saw) application for teleoperated surgical robot system. The MIDAS Journal-Systems and Architectures for Computer Assisted Interventions, 2009.
- [10] Anton Deguet, Rajesh Kumar, Russell Taylor, and Peter Kazanzides. The cisst libraries for computer assisted intervention systems. In MICCAI Workshop on Systems and Arch. for Computer Assisted Interventions, Midas Journal, 2008.

- [11] Zhixian Zhang, Adnan Munawar, and Gregory S Fischer. Implementation of a motion planning framework for the davinci surgical system research kit. In *The Hamlyn Symposium on Medical Robotics*, page 43, 2014.
- [12] Sachin Chitta, Ioan Sucan, and Steve Cousins. Moveit![ROS topics]. Robotics & Automation Magazine, IEEE, 19(1):18–19, 2012.
- [13] Jia Pan, Sachin Chitta, and Dinesh Manocha. FCL: A general purpose library for collision and proximity queries. In *Robotics and Automation* (ICRA), 2012 IEEE International Conference on, pages 3859–3866. IEEE, 2012.
- [14] Joseph Luk, Jerome Pasquero, Shannon Little, Karon MacLean, Vincent Levesque, and Vincent Hayward. A role for haptics in mobile interaction: initial design using a handheld tactile display prototype. In *Proceedings of the SIGCHI conference on Human Factors in computing systems*, pages 171–180. ACM, 2006.
- [15] Brian T Bethea, Allison M Okamura, Masaya Kitagawa, Torin P Fitton, Stephen M Cattaneo, Vincent L Gott, William A Baumgartner, and David D Yuh. Application of haptic feedback to robotic surgery. *Journal of Laparoendoscopic & Advanced Surgical Techniques*, 14(3):191–195, 2004.
- [16] Allison M Okamura. Methods for haptic feedback in teleoperated robot-assisted surgery. *Industrial Robot: An International Journal*, 31(6):499–508, 2004.
- [17] Fredrik Ryden, Sina Nia Kosari, and Howard Jay Chizeck. Proxy method for fast haptic rendering from time varying point clouds. In Intelligent Robots and Systems (IROS), 2011 IEEE/RSJ International Conference on, pages 2614–2619. IEEE, 2011.
- [18] EP Westebring-Van Der Putten, RHM Goossens, JJ Jakimowicz, and J Dankelman. Haptics in minimally invasive surgery-a review. Minimally Invasive Therapy & Allied Technologies, 17(1):3–16, 2008.
- [19] Mandayam A Srinivasan and Cagatay Basdogan. Haptics in virtual environments: Taxonomy, research status, and challenges. *Computers & Graphics*, 21(4):393–404, 1997.
- [20] Bruno Siciliano and Luigi Villani. Robot force control, volume 540. Springer Science & Business Media, 2012.
- [21] J Edward Colgate and J Michael Brown. Factors affecting the z-width of a haptic display. In *Robotics and Automation*, 1994. Proceedings., 1994 IEEE International Conference on, pages 3205–3210. IEEE, 1994.